Original Article

MOLECULAR METABOLISM

ABHD6 suppression promotes anti-inflammatory polarization of adipose tissue macrophages via 2-monoacylglycerol/PPAR signaling in obese mice

P. Poursharifi [1,*], C. Schmitt [1], I. Chenier [1], Y.H. Leung [1], A.K. Oppong [1], Y. Bai [1], L.-L. Klein [1], A. Al-Mass [2], R. Lussier [1], M. Abu-Farha [3], J. Abubaker [3], F. Al-Mulla [3], M.-L. Peyot [1], S.R.M. Madiraju [1], M. Prentki [1,**]

ABSTRACT

Objective: Pro-inflammatory polarization of adipose tissue macrophages (ATMs) plays a critical role in the pathogenesis of obesity-associated chronic inflammation. However, little is known about the role of lipids in the regulation of ATMs polarity and inflammation in response to metabolic stress. Deletion of α/β-hydrolase domain-containing 6 (ABHD6), a monoacylglycerol (MAG) hydrolase, has been shown to protect against diet-induced obesity and insulin resistance.

Methods: Here we investigated the immunometabolic role of macrophage ABHD6 in response to nutrient excess using whole-body ABHD6-KO mice and human and murine macrophage cell-lines treated with KT203, a selective and potent pharmacological ABHD6 inhibitor.

Results: KO mice on high-fat diet showed lower susceptibility to systemic diet-induced inflammation. Moreover, in the setting of overnutrition, stromal vascular cells from gonadal fat of KO *vs.* control mice contained lower number of M1 macrophages and exhibited enhanced levels of metabolically activated macrophages (MMe) and M2 markers, oxygen consumption, and interleukin-6 (IL-6) release. Likewise, under *in vitro* nutri-stress condition, inhibition of ABHD6 in MMe-polarized macrophages attenuated the expression and release of pro-inflammatory cytokines and M1 markers and induced the upregulation of lipid metabolism genes. ABHD6-inhibited MMe macrophages showed elevated levels of peroxisome proliferator-activated receptors (PPARs) and 2-MAG species. Notably, among different MAG species, only 2-MAG treatment led to increased levels of PPAR target genes in MMe macrophages.

Conclusions: Collectively, our findings identify ABHD6 as a key component of pro-inflammatory macrophage activation in response to excess nutrition and implicate an endogenous macrophage lipolysis/ABHD6/2-MAG/PPARs cascade, as a lipid signaling and immunometabolic pathway, which favors the anti-inflammatory polarization of ATMs in obesity.

Keywords α/β-hydrolase domain-containing 6; Monoacylglycerol; Immunometabolism; Inflammation; Lipid metabolism; Macrophage

1. INTRODUCTION

Macrophages are a heterogeneous group of innate immune cells with essential roles in metabolism, host defense, and tissue and organismal homeostasis [1]. An imbalance in macrophage polarization occurs in both acute and chronic inflammatory settings, such as infection and metabolic stress [2]. Bacterial endotoxin lipopolysaccharide (LPS) or interferon-γ (IFN-γ) induce the classical activation of macrophages (M1-type), which is characterized by the overproduction of pro-inflammatory cytokines that can harm the host tissues. Conversely, interleukin-4 (IL-4) promotes alternative (M2-type) macrophage polarization with the mission to resolve inflammation and to maintain tissue and nutrient homeostasis [3,4].

Chronic low-grade inflammation in metabolic tissues, such as white adipose tissue (WAT), results in immunometabolic imbalance, which leads to insulin resistance and obesity-related complications [5–8]. The increased number of AT macrophages (ATMs) in obesity has been conventionally attributed to a simplistic pathologic switch of anti-inflammatory (M2-like) to pro-inflammatory (M1-like) ATMs [9]. Currently, the M1-/M2-like paradigm in AT inflammation is evolving as a result of the identification of new ATM subpopulations [10–12]. In fact, it has been shown recently that obesity reprograms ATMs to a

[1]Montreal Diabetes Research Center - Centre de Recherche du Centre Hospitalier de l'Université de Montréal, Montreal, Canada [2]Department of Biological Sciences, Faculty of Science, Kuwait University, Kuwait City, Kuwait [3]Dasman Diabetes Institute, Kuwait City, Kuwait

*Corresponding author. Montreal Diabetes Research Center, CRCHUM, Viger Tower, 900 Saint Denis St, R-08-476, Montreal, QC, H2X 0A9, Canada. Tel.: +1 514 890 8000x30176. E-mail: pegah.poursharifi.chum@ssss.gouv.qc.ca (P. Poursharifi).

**Corresponding author. Montreal Diabetes Research Center, CRCHUM, Viger Tower, 900 Saint Denis St, R-08-436, Montreal, QC, H2X 0A9, Canada. Tel.: +1 514 890 8000x23642. E-mail: marc.prentki@umontreal.ca (M. Prentki).

Received July 25, 2023 • Revision received September 25, 2023 • Accepted October 8, 2023 • Available online 12 October 2023

https://doi.org/10.1016/j.molmet.2023.101822

pro-inflammatory metabolically activated state (MMe), which is mechanistically, functionally and transcriptionally distinct from the M1- or M2-like phenotypes [13]. To complicate things further, it has been proposed that the MMe possess a unique pleiotropic phenotype in AT health, which fluctuates between being beneficial (clearing dead adipocytes) and detrimental (secreting pro-inflammatory cytokines) depending on the duration of high-fat feeding [14]. Importantly, MMe macrophages have been implicated in nutri-stress conditions *in vitro* [13], as well as *in vivo,* in obesogenic ATMs from mice and human WAT [13,14] and in mammary AT promoting tumorigenesis during obesity [15]. Despite these advances in our understanding of the diversity and functions of ATMs, the underlying molecular pathways regulating the relationship between the metabolic phenotype and inflammatory properties of ATMs are still poorly understood.

Macrophages are equipped with complex mechanisms to efficiently uptake, store, breakdown, oxidize and liberate lipids [16]. In fact, the earlier view in which pro-inflammatory macrophages solely rely on glucose, but not lipid metabolism, is currently being reexamined [17]. A consensus is yet to be found, but a number of studies have highlighted the importance of exogenous and endogenous lipids in the polarization and function of pro-inflammatory macrophages [18–21]. Accordingly, it is currently appreciated that modulating macrophage lipid metabolism is an effective strategy to tackle inflammation [17].

Previous studies have highlighted the importance of monoacylglycerol (MAG), which can be hydrolyzed by monoacylglycerol lipase (MAGL), α/β-hydrolase domain-containing 6 (ABHD6) and ABHD12, as a signaling competent lipid [22]. ABHD6, which was first identified in the brain [23], is a ubiquitously expressed lipase [22] and its biochemical and physiological functions in different tissues are only being revealed recently. Using global and tissue-specific ABHD6 knockout (KO) models, our group has studied the metabolic and signaling roles of ABHD6 and its substrate MAG in pancreatic insulin secretion [24,25], AT browning and obesity [26] and cold-induced thermogenesis [27]. The beneficial effects of ABHD6 suppression have been attributed to the MAG signaling through its cellular targets, such as mammalian Unc13-1, cannabinoid receptors, GPR119 and peroxisome proliferator-activated receptors (PPARs) [22]. Several initial studies have demonstrated that pharmacological blockade of ABHD6 results in elevated levels of the endocannabinoid 2-arachidonylglycerol (2-AG), which exerts anti-inflammatory effects in LPS-stressed macrophages with potential therapeutic implications in the context of neuroinflammation [28–31]. Nevertheless, these observations are yet to be confirmed *in vivo* with transgenic animal models to avoid potential off-target effects of ABHD6 inhibitors [32,33]. Besides, all of these studies have investigated the inflammation regulatory role of ABHD6 and 2-AG solely in response to the classical stimulus LPS and/or other infectious agents, but not under metabolic nutrient-excess stress (nutri-stress) [34], without microbial inflammation.

Here we combine pharmacological and genetic approaches to investigate the inflammation regulatory roles of ABHD6 during nutri-stress condition. The results identify ABHD6 as a positive modulator of pro-inflammatory macrophage activation and implicate a lipolysis/ABHD6/2-MAG/PPARs cascade, possibly in conjunction with NADPH-oxidase-2 (NOX2)/interleukin-6 (IL-6)/signal transducer and activator of transcription 3 (STAT3)/arginase 1 (Arg1) signaling, as an important immunometabolic pathway, which favors the anti-inflammatory polarization of ATMs in obesity.

2. MATERIALS AND METHODS

Study models and chemical/biological materials are summarized in Supplemental Table 1.

2.1. Animal studies

Mice were maintained in the local animal facility at a 12 h light/dark cycle with free access to food and water. Whole-body ABHD6-KO (KO) mice on pure C57BL/6N genetic background were generated as described previously [24]. There are sex-associated differences in the pattern of obesity-induced inflammation in humans, where excessive production of pro-inflammatory mediators is more prominent in men, while women exhibit reduced levels of the anti-inflammatory adipokine adiponectin [37]. Several preclinical studies in rodents have shown that females are protected against HFD-induced inflammation [38–41] and therefore here we employed male mice. At weaning, KO and WT mice were housed individually and were placed on a 60% high-fat diet (HFD; Research Diet #D12492) for 17 weeks. Body weight and food intake were measured weekly. All the procedures for mouse studies were performed in accordance with the Institutional Committee for the Protection of Animals at the Université de Montréal Hospital Research Center (CRCHUM).

2.2. Cells/macrophages

All cell cultures were incubated at 37 °C, with 5% CO_2 in a humidified atmosphere.

RAW264.7 and J774 cells were cultured in Dulbecco's modified Eagle's medium (DMEM) and Roswell Park Memorial Institute 1640 (RPMI-1640), respectively. Cell culture media were supplemented with 10% (*v/v*) fetal bovine serum (FBS) and antibiotics. Cells were passaged when they became 70%–80% confluent and media was changed every 2–3 days.

The human monocytic cell line (THP-1) was grown in RPMI-1640, supplemented with 10% (*v/v*) fetal bovine serum (FBS), 10 mM HEPES, 1 mM sodium pyruvate/0.05 mM 2-mercaptoethanol and antibiotics. Cells were then treated with phorbol-12-myristate 13-acetate (PMA) (100 ng/mL) for 48 h to allow differentiation. The adherent macrophages were used for experiments after 24 h. Differentiation was ascertained by assessing the mRNA expression of the macrophage marker *CD68* (data not shown).

Peritoneal macrophages (PMs) were isolated from WT and KO male mice as described [35]. In brief, PMs were obtained by peritoneal lavage and plated in the presence of DMEM medium supplemented with 10% (*v/v*) FBS and antibiotics.

At the end of the HFD protocol, stromal vascular fraction (SVF) cells were isolated from visceral perigonadal white adipose tissue (gWAT), subcutaneous inguinal WAT (iWAT) and interscapular brown AT (iBAT). Concisely, harvested fat pads were minced, washed, and then digested in collagenase type II (1 mg/mL in Krebs Ringer Buffer Hepes (KRBH) supplemented with 2% fatty acid–free BSA) for 30 min at 37 °C. Floating mature adipocytes were collected for gene expression, TG and protein assessments and lipolysis. The SVF pellet was washed, depleted of red blood cells, filtered and re-suspended in various buffers or media, depending on the subsequent analysis.

2.3. Polarization of macrophages

For MMe polarization, M0 (non-activated/untreated) macrophages were treated with glucose (30 mM), insulin (10 nM) and palmitate (0.4 mM) for 24 h [13]. The ABHD6 inhibitor (KT203 (10 μM)) was added 1 h before the polarization treatments. Activated macrophages, along with the untreated cells (M0), were then subjected to analysis by qRT-PCR, immunoblotting, cytokine/lactate release, migration assay, TG content, MAG species analysis, etc.

2.4. Cytokine release

MMe-polarized macrophages and SVF cells were cultured for 24 h. The cell culture supernatants were collected, centrifuged and the concentrations of IL-6, MCP1 and TNFα were determined by using available commercial kits (Supplemental Table 1), following the manufacturer's instructions. Adherent cells were then washed and collected for protein measurement and normalization.

2.5. Seahorse bioenergetic measurements

Real-time oxygen consumption rate (OCR) measurements in SVF cells were made with a XF24 Analyzer (Seahorse Bioscience) as previously described [18] with slight modifications. In brief, freshly isolated SVF cells were plated into each well of Seahorse cell culture plates and allowed adherence for at least 2 h before treatment. For assessing the respiratory capacity, cells were subjected to pre-incubation at 37 °C for a minimum of 30 min in the absence of CO_2. The Seahorse assay buffer was supplemented with 25 mM glucose, 2 mM glutamine, 1 mM sodium pyruvate and 0.5% free-fatty acid BSA. After three basal OCR measurements, compounds (1.5 μM Oligomycin; 5 μM fluoro-carbonyl cyanide phenylhydrazone (FCCP); 2 μM Antimycin A and 1 μM Rotenone) were sequentially injected into the plate. Basal respiration was calculated by subtracting the average of the post-Antimycin A and Rotenone measurements from the average of the first three measurements.

2.6. Lipolysis

Lipolysis was assessed as described previously [27].

2.7. TG content

Tissues were homogenized in ice-cold lysis buffer (20 mM Tris-HCl, pH 7.2, containing 150 mM NaCl, 1 mM EDTA, 1 mM EGTA, 1% (v/v) Triton X-100, 0.1% SDS) and then assayed for TG using available commercial colorimetric kit (Supplemental Table 1). TG values were normalized by protein content.

Freshly isolated mature adipocytes were carefully collected and equal amount of packed adipocytes were aliquoted into two tubes. One tube proceeded to lipid extraction and TG assessment and the other aliquot was used for protein measurement. TG values were normalized by protein content.

2.8. Lipidomics

Analysis of different species of 1- and 2-MAG was done as described previously [26,27].

2.9. Immunoblotting

Proteins were extracted using ice-cold lysis buffer (20 mM Tris-HCl, pH 7.2, containing 150 mM NaCl, 1 mM EDTA, 1 mM EGTA, 1% (v/v) Triton X-100, 0.1% SDS, and protease inhibitors). After protein quantification, 25–40 μg protein was used for western blot analysis. Antibodies are listed in Supplemental Table 1.

2.10. Flow cytometry

Flow cytometry analyses of macrophage subtypes using freshly isolated SVF cells were performed as described [36] with minor modifications. Dead cells were labeled using LIVE/DEAD™ Fixable Aqua Dead Cell Stain Kit. Fluorophore-coupled primary antibodies and dilutions are listed in Supplementary Table 1. For analysis of flow cytometry data, after elimination of cell aggregates and dead cells, viable cells were gated for adipose tissue leukocytes ($CD45^+$ cells). Subsequently, $CD45^+CD11b^+F4/80^+$ cells were defined as ATMs. As recommended [36], to minimize contamination with other cell types only $F4/80^{hi}$ population was selected for assessment of surface expression of CD11c (M1 marker) and CD301 (M2 marker). Analysis was performed using a BD Fortessa flow cytometer equipped with FACSDiva software. Quantification was done using FlowJo v10.7 software. Compensation was performed using single stain and fluorescence-minus-one controls, as well as compensation beads.

2.11. Cytokine proteome profiler array

Plasma samples were run in duplicates with a MILLIPLEX MAP Mouse Cytokine/Chemokine kit according to the manufacturer's instructions. The kit simultaneously quantified multiple cytokines and chemokines with Bead-based Multiplex assays using the Luminex technology.

2.12. Tissue histology and analysis

Freshly dissected gWAT, iWAT and iBAT were fixed in 10% paraformaldehyde in PBS, dehydrated, embedded in paraffin and sectioned. Sections were stained with hematoxylin and eosin (H&E). Images were processed for cell size and number as previously detailed [27].

2.13. RNA isolation and analysis

Total RNA was isolated from tissues and cells using the RNeasy Mini Kit according to the manufacturer's instructions (Qiagen). Following reverse-transcription of 2 μg RNA to cDNA, gene expression was determined by qPCR using SYBR Green. All gene expression analyses were run in duplicate and normalized to either *18s* or *Gapdh*. Primer sequences are listed in the Supplemental Table 2.

2.14. Statistical analysis

Graphs were plotted and data were analyzed by GraphPad Prism 9.4.1. Results are expressed as means ± SEM. Normal distribution of the data was tested with the Gaussian distribution test. Statistical differences between 2 groups were assessed by unpaired 2-tailed Student's t test when data were normally distributed. The Mann Whitney test was used for nonparametric data. For statistical analysis among multiple groups, 1-way or 2-way ANOVAs were used, as indicated. A *P* value of less than 0.05 was considered statistically significant.

3. RESULTS

3.1. Pan-deletion of ABHD6 limits high-fat diet-induced systemic inflammation

In the present study, we determined whether ABHD6 suppression protects against diet-induced chronic inflammation, in addition to the previously recognized beneficial effects of global ABHD6 deletion against obesity, glucose intolerance, insulin resistance and hyperinsulinemia [26]. Whole body ABHD6-KO and WT mice were exposed to a high-fat diet (HFD) regimen (60% calories from fat) for 17 weeks, starting after weaning. Consistent with our previous study [26], at the end of HFD protocol, ABHD6-KO gained ~12% less body weight than WT mice ($p = 0.01$; data not shown).

Cytokine proteome profiler array revealed lower levels of pro-inflammatory chemokines/cytokines (CXCL1 and IL1α), and upregulation of VEGF in the plasma of HFD-fed ABHD6-KO versus WT mice (Figure 1A). Trends of changes ($p = 0.1$) towards increased IL-6 and decreased CXCL5 and CXCL10 were also noticed. Large hypertrophic adipocytes (>70 μm in diameter) in obesity are metabolically dysfunctional and less responsive. These cells are associated with insulin resistance and inflammation-related pathological conditions, unlike the smaller adipocytes [42]. Fat pads from HFD fed ABHD6-KO mice, compared to WT mice, contained smaller adipocytes

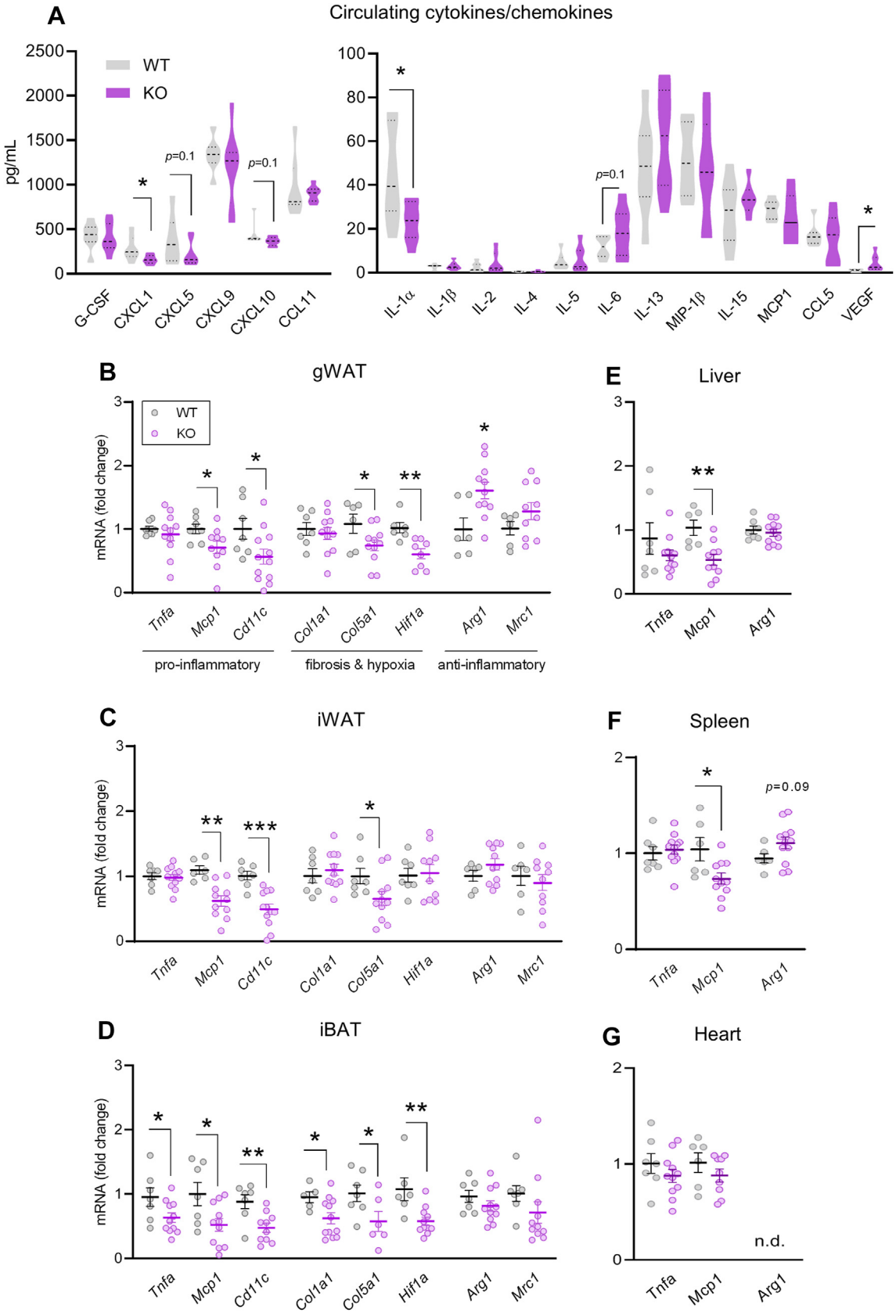

Figure 1: Pan-deletion of ABHD6 limits high-fat diet-induced systemic inflammation. At weaning, male KO and WT mice were housed individually and were placed on a 60% high-fat diet for 17 weeks. **(A)** Plasma cytokine and chemokine array. **(B–G)** The mRNA levels of pro-/anti-inflammatory and/or fibrosis/hypoxia markers. Minimum 7 mice/group. Student's t test; $^{*}p < 0.05$, $^{**}p < 0.01$, $^{***}p < 0.001$.

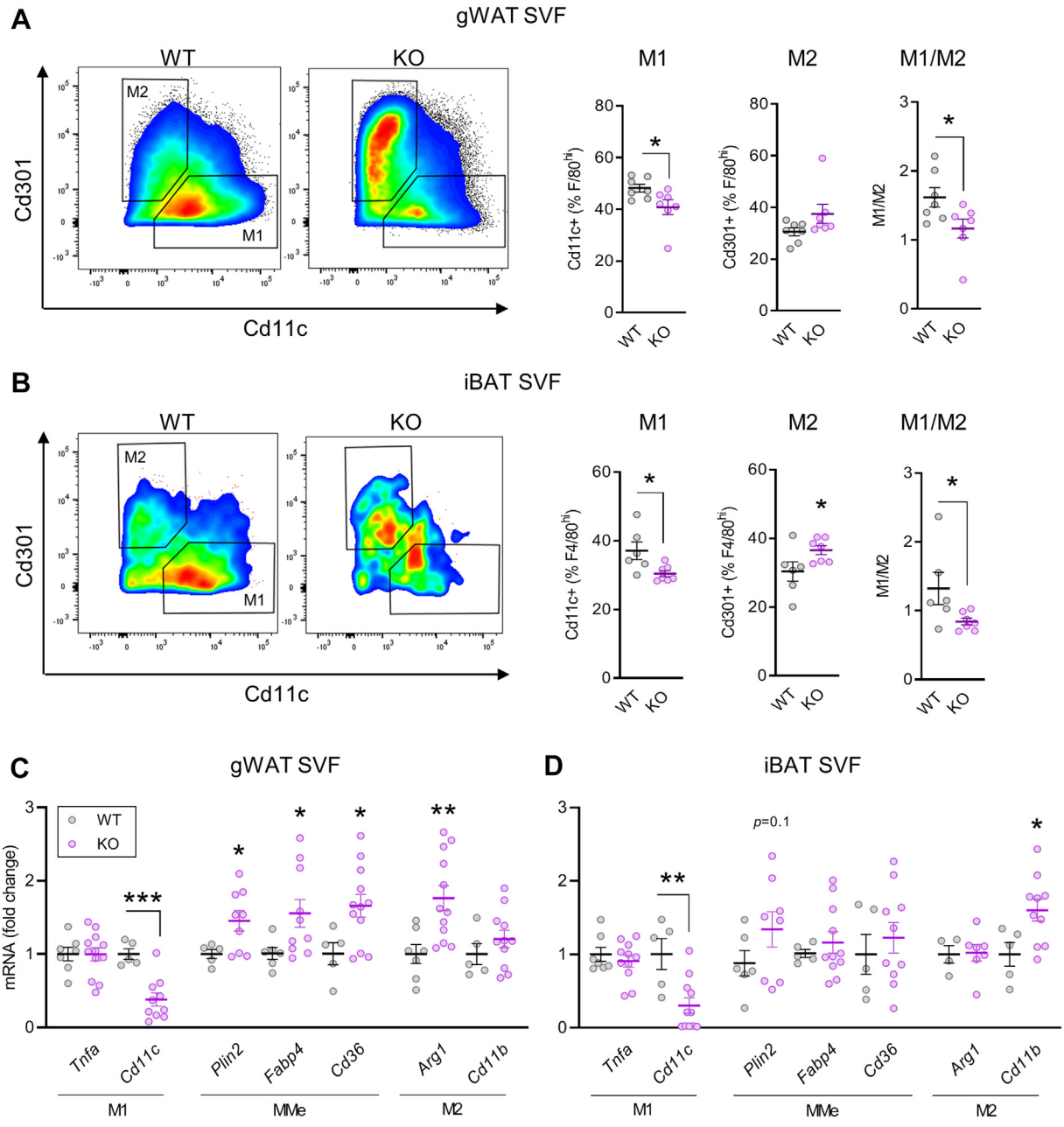

Figure 2: Pan-deletion of ABHD6 limits high-fat diet-induced inflammation in the visceral and brown fat and decreased the number of M1-like ATMs. At the end of the HFD regimen, stromal vascular fraction (SVF) cells were isolated from fat depots and were subjected to flow cytometry or RNA isolation procedures. **(A** and **B)** Representative plots and quantification of flow cytometry for M1 ($F4/80^{hi}CD11c^{+}CD301^{-}$ cells) and M2 ($F4/80^{hi}CD11c^{-}CD301^{+}$ cells) adipose tissue macrophages (ATMs, $CD45^{+}CD11b^{+}F4/80^{+}$ cells) in fat depots, and M1-like/M2-like ratio (n = 6, each group). **(C** and **D)** The mRNA levels of M1, MMe and M2 markers. Minimum 6 mice/group. **(A** and **B)** Mann Whitney test; **(C** and **D)** Student's t test; $*p < 0.05$, $**p < 0.01$, $***p < 0.001$.

(Figure S1a) with lower mRNA levels of pro-inflammatory, fibrosis and hypoxia markers (Figure 1B—D). The anti-inflammatory marker *Arg1* was significantly elevated in the gonadal fat (gWAT) of ABHD6-KO vs WT mice (Figure 1B). *Mcp1* mRNA expression was reduced in the liver (Figure 1E) and spleen (Figure 1F) of the ABHD6-KO mice, but only a trend of reduction was noticed in the heart (Figure 1G).

Chronic nutri-stress causes dysregulation of systemic lipid metabolism, which leads to ectopic fat accumulation and a vicious cycle of deteriorated immuno-metabolic regulation [43]. Under HFD, ABHD6-KO mice compared to the WT, showed lower accumulation of triglyceride (TG) in the liver and spleen (Figure. S1b). Accordingly, the weights of liver, spleen and heart were lower in HFD-fed ABHD6-KO versus WT mice (Figure S1c). Besides, significant decrease in TG content was observed in the isolated mature adipocytes from KO iBAT versus WT, but not in iWAT and gWAT depots (Figure S1d).

Obesity and associated insulin resistance/inflammation upregulate basal lipolysis, yet suppress adrenergic receptor signaling in white adipocytes [44,45]. To further examine if ABHD6 deletion, in addition to exerting anti-inflammatory effects, also influences lipolysis in adipocytes, isolated mature adipocytes from HFD-fed mice were treated

with β-adrenergic receptor agonist isoproterenol (ISO). No differences were observed between groups in basal lipolysis of white adipocytes, but ISO-stimulated release of glycerol and non-esterified fatty acids (NEFA) were significantly higher in the ABHD6-KO gWAT adipocytes versus control (Figure S1e). Also, ABHD6-KO adipocytes from inguinal fat (iWAT) exhibited elevated ISO-stimulated NEFA release, compared to the WT (Figure S1f). In addition, ABHD6-KO brown adipocytes showed increased basal glycerol and NEFA release compared to the WT (Figure S1g), consistent with their decreased TG content (Figure S1d). Thus, ABHD6 deletion prevents the HFD-induced dysregulation of lipid metabolism and lipolysis in WAT, which may likely play a role in curtailing HFD-induced systemic inflammation.

3.2. Pan-deletion of ABHD6 limits high-fat diet-induced inflammation in the visceral and brown fat and decreases the number of M1-like ATMs

In obesity macrophages are the most abundant innate immune cells that infiltrate and accumulate in AT and contribute to a state of low-grade chronic inflammation and impaired metabolism [46]. To further investigate the involvement of ABHD6 in the regulation of diet-induced AT inflammation, we analyzed the macrophage content/subsets in the stromal vascular fraction (SVF) from HFD-fed ABHD6-KO and WT mice by flow cytometry using CD45, F4/80, CD11b, CD11c and CD301 markers [18,36] (see Figure S2a for gating strategy). Flow cytometry analysis showed comparable number of $CD45^+$ cells in the gWAT and iWAT, but significantly less $CD45^+$ cells in the interscapular brown AT (iBAT) SVF from KO *vs* WT mice (Figure S2b). There was no difference in the distribution of $CD45^+F4/80^+CD11b^+$ cells (ATMs) between KO and WT in all fat depots, with an expected higher proportion of ATMs within SVF cells in gWAT (~45%), compared to the iWAT (~22%) and iBAT (~20%) (Figure S2c). Within the $F4/80^{hi}CD11b^+$ ATM population, we identified a significant decrease in the percentage of $CD11c^+CD301^-$ cells (M1-like ATMs) in both gWAT (Figure 2A) and iBAT (Figure 2B), thus causing a marked decline in the M1/M2 ratio (Figure 2A,B). Further, the percentage of $CD11c^-CD301^+$ cells (M2-like ATMs) was higher in the iBAT from ABHD6-KO mice compared to WT (Figure 2B). No significant changes were found in the M1-and M2-like ATMs within the iWAT depot of KO versus WT mice (Figure S2d).

Transcriptional analysis using isolated SVF cells yielded results consistent with those of the flow cytometry. Thus, M1-like marker, *Cd11c*, was drastically downregulated, while 'metabolically activated' (MMe) (*Plin2*, *Fabp4*, *Cd36* [13]) and M2 (*Arg1*) markers were all upregulated in the gWAT SVF from ABHD6-KO *vs* WT mice (Figure 2C). Compared to the WT, iBAT SVF from ABHD6-KO mice also showed a marked decrease in *Cd11c* expression and a significant upregulation of *Cd11b*, with no changes in MMe markers (Figure 2D). Recently, another subpopulation of ATMs, triggering receptor expressed on myeloid cells 2 $(Trem2)^+$ lipid-associated macrophages (LAM), have been implicated in the obesity-related complications [47]. To study the possible role of ABHD6 in regulating LAM macrophages in obesity, we have assessed the mRNA expression of *Trem2* in the ATs and SVF cells from HFD-fed KO versus WT mice. Based on our data, *Trem2* was highly expressed in the gWAT compared to the iWAT and iBAT depots (in the ATs (Figure S2e) and the corresponding SVF cells (Figure S2f)). The results shown that *Trem2* is downregulated in the BAT of ABHD6-KO mice, yet no differences were found in the WATs (Figure S2e). Further, as illustrated in Figure S2f, *Trem2* levels were comparable between KO and WT SVF cells. Therefore, the observed decrease in *Trem2* expression in the BAT (Figure S2e) could be due to its expression in adipocytes or other cells, rather than macrophages.

Overall, while the anti-inflammatory effects of ABHD6 deletion observed in gWAT SVF were largely mirrored in the brown fat SVF, the changes in the gonadal depot were more prominent. This prompted us to compare gWAT *vs.* iWAT *vs.* iBAT *Abhd6* mRNA levels using whole AT lysates and SVF cells. In the HFD-fed mice, although iBAT, compared to the gWAT and iWAT, harbors more *Abhd6* level, the expression of *Abhd6* in SVF is significantly higher in the gWAT and iWAT (Figure S2g). Hence, there are depot-specific differences in the immunometabolic profile of ABHD6-KO ATMs across fat depots, with more favorable changes in the gWAT SVF/ATMs, which normally have higher *Abhd6* expression. Further, despite the high expression of *Abhd6* in the iWAT SVF, there were no substantial changes in the inflammation of iWAT depot comparing KO and WT, which may suggest other roles, rather than inflammation, for ABHD6 in this depot.

3.3. ABHD6 contributes to MAG lipolysis in gWAT and iBAT SVF cells during obesity

To study the role of ABHD6 in ATM metabolism in the context of obesity, we measured oxygen consumption rate (OCR) and lactate release, as well as TG content and lipolysis of freshly isolated SVF cells of HFD-fed WT and ABHD6-KO mice. We found significantly higher basal OCR in the gWAT-SVF cells from ABHD6-KO versus WT mice, though no differences were found in lactate release or TG content (Figure 3 a-c). Although the expression of lipolytic enzymes (*Atgl*, *Hsl* and *Mgll*) in gWAT-SVF was unchanged (Figure 3D), ABHD6-KO SVF cells released less glycerol and FFA compared to WT (Figure 3E), which indicates a contribution of ABHD6 to MAG hydrolysis, besides that of MAGL.

Unfortunately we were not able to measure OCR in iBAT-SVF cells, probably due to the low yield/cell density, and also remarkably distinct cell populations of iBAT compared to the WAT SVF [48]. Lactate release from iBAT SVF, regardless of glucose concentration, was not significantly changed between the two groups (Figure 3F). Notably, ABHD6-deficient iBAT-SVF exhibited lower TG content, compared to the WT (Figure 3G). Similar to gWAT-SVF, KO iBAT-SVF exhibited significantly reduced glycerol and NEFA release (Figure 3H), yet no changes were observed in the mRNA levels of lipolytic enzymes (Figure 3I). There were no differences between KO and WT iWAT-SVF either in TG content or in glycerol/NEFA release (Figure 3a and b).

Together, these data demonstrate that ABHD6 contributes to MAG lipolysis in HFD visceral and brown fat SVF cells and its deletion in gWAT-SVF reprograms macrophage metabolism to adopt high basal respiratory capacity, without alterations in glucose metabolism, correlated with their anti-inflammatory properties [49].

3.4. ABHD6 suppression or inhibition in MMe macrophages upregulates lipid metabolism genes and reduces pro-inflammatory markers

As SVF contains a variety of cell types, to better investigate the immunometabolic state of ABHD6-suppressed macrophages during nutri-stress, we used murine and human monocyte/macrophage cell lines. To generate diet-induced inflammation *in vitro*, macrophage cell-lines were polarized into MMe state [13]. Continuous exposure to free fatty acids (FFA) drives MMe phenotype polarization by two independent pathways: FFA/toll-like receptors (TLRs), which drive pro-inflammatory cytokine production, and FFA/PPARγ and the autophagy-associated protein p62, which induce lipid metabolism pathways [13]. Notably, M2 markers are suppressed or not expressed in MMe macrophages *in vitro* [13]. Likewise, in our experimental setting, polarization of RAW 264.7 and THP1 macrophages into MMe by incubation with palmitate/glucose/insulin induced the upregulation

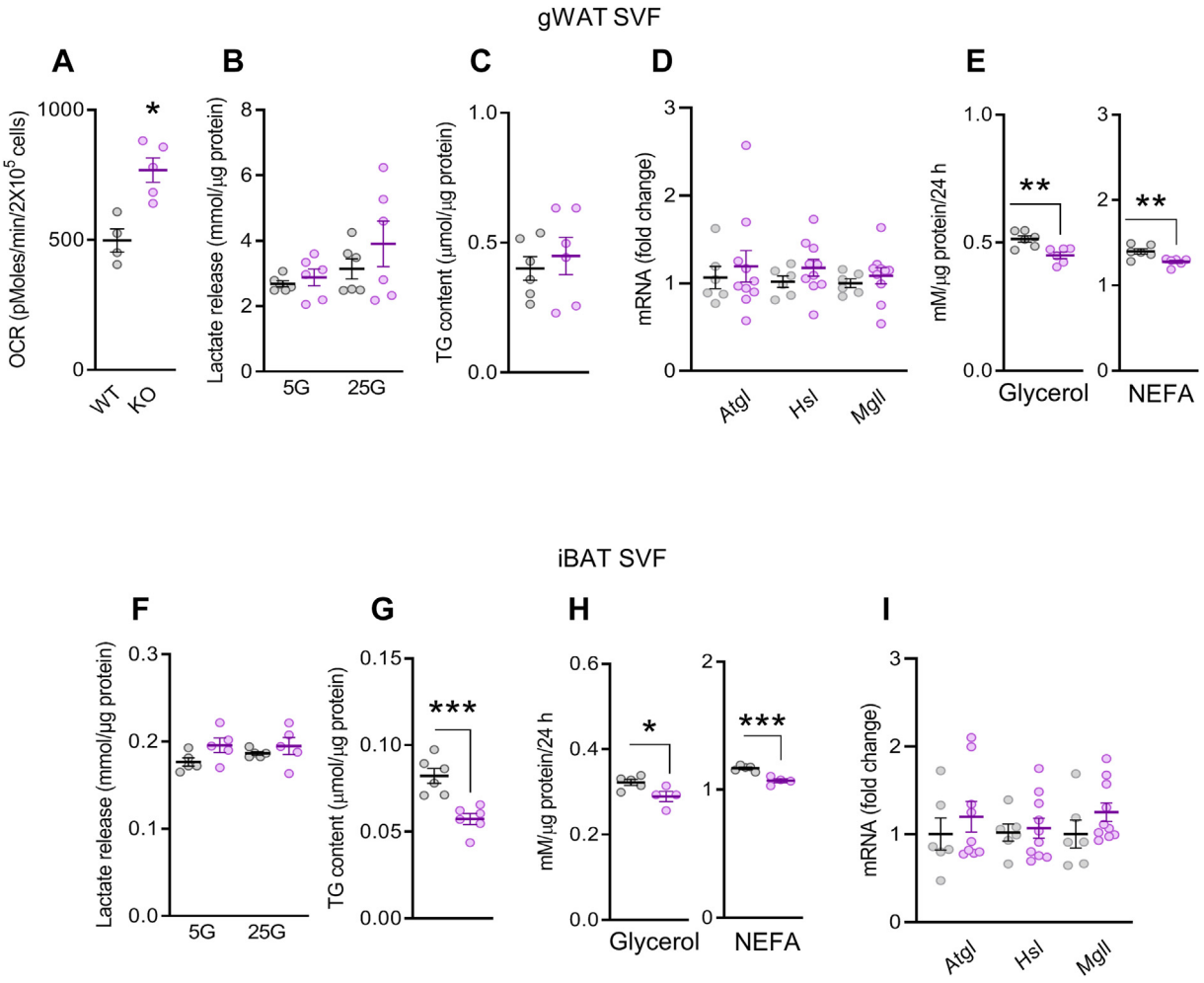

Figure 3: ABHD6 contributes to MAG lipolysis in gWAT and iBAT SVF cells during obesity. At the end of the HFD regimen, stromal vascular fraction (SVF) cells were isolated from fat depots and were used in various experiments. **(A)** Basal oxygen consumption rate (OCR) level. **(B** and **F)** Lactate release. **(C** and **G)** TG content. **(D** and **I)** The mRNA expression of lipolytic enzymes. **(E** and **H)** Glycerol and NEFA release. 4–10 mice/group. Student's t test; $*p < 0.05$, $**p < 0.01$, $***p < 0.001$.

of both lipid metabolism and pro-inflammatory associated genes (Figure 4a and b), yet as reported before [13], M2 markers were expressed at very low levels (data not shown).

To inhibit ABHD6 activity, MMe macrophages were treated with KT203 (IC50, 0.82 nM [50]), which is a much more selective and potent pharmacological ABHD6 inhibitor than the previously used WWL70 (IC50, 55 nM [32]) [28]. In fact, the near complete inhibitory effect of KT203 against ABHD6 has been reported earlier *in vitro* using Neuro2A cells and *in vivo* in mice [50]. Inhibition of ABHD6 in MMe-polarized murine macrophage cell line, RAW 264.7, led to lower intracellular lipid accumulation (Figure 4A,B), less release (Figure 4C) and expression (Figure 4D) of pro-inflammatory TNFα and MCP1 cytokines, yet significantly higher levels of lipid metabolism related genes (*Plin2*, *Fabp4*, *Cd36* and *Cpt1a*), compared to vehicle treated cells (Figure 4D). Compatible with their pro-inflammatory properties, MMe macrophages released more lactate compared to the unstimulated macrophages (M0); however, KT203 had no effect on lactate release by MMe cells (Figure S4c). Moreover, inhibition of ABHD6 with KT203 in human macrophages (THP1) (Figure 4E) and deletion of ABHD6 (KO) in primary mouse peritoneal macrophages (Figure 4F) resulted in the down-regulation of pro-inflammatory markers and upregulation of genes associated with lipid metabolism. Next, we have assessed if the expression of *Trem2* (LAM marker [47]) is altered with ABHD6 inhibition in MMe-polarized RAW 264.7 macrophages *in vitro*. As shown in Figure S4d, *Trem2* expression was higher in MMe compared to the M0 macrophages; yet, ABHD6 inhibition had no effect on *Trem2* mRNA level in the MMe macrophages. Finally, mRNA expression of *Gapdh* (used as a reference gene for the cell-lines) (Figure S4e) revealed stable levels among KT203-treated and untreated M0 and MMe RAW 264.7 cells.

Collectively, our *in vitro* and *ex vivo* data suggest that inhibition or deletion of ABHD6 in MMe macrophages limits pro-inflammatory pathways and promotes more anti-inflammatory phenotype characterized by enhanced lipid metabolism [13,49].

3.5. ABHD6 inhibition promotes 2-MAG/PPARγ and α signaling in macrophages

We investigated the mechanism by which ABHD6 suppression alleviates the inflammatory responses in macrophages. In order to assess whether MAG-mediated signaling is involved, we first treated MMe macrophages, derived from RAW264.7 cells, with exogenous MAG species (1-oleoylglycerol (1-OG), 2-OG and 2-AG), as well as agonists of PPARα (WY-14643 (WY)) and PPARγ (pioglitazone (Pio)). Consequently, the levels of inflammatory cytokines, MMe and LAM markers,

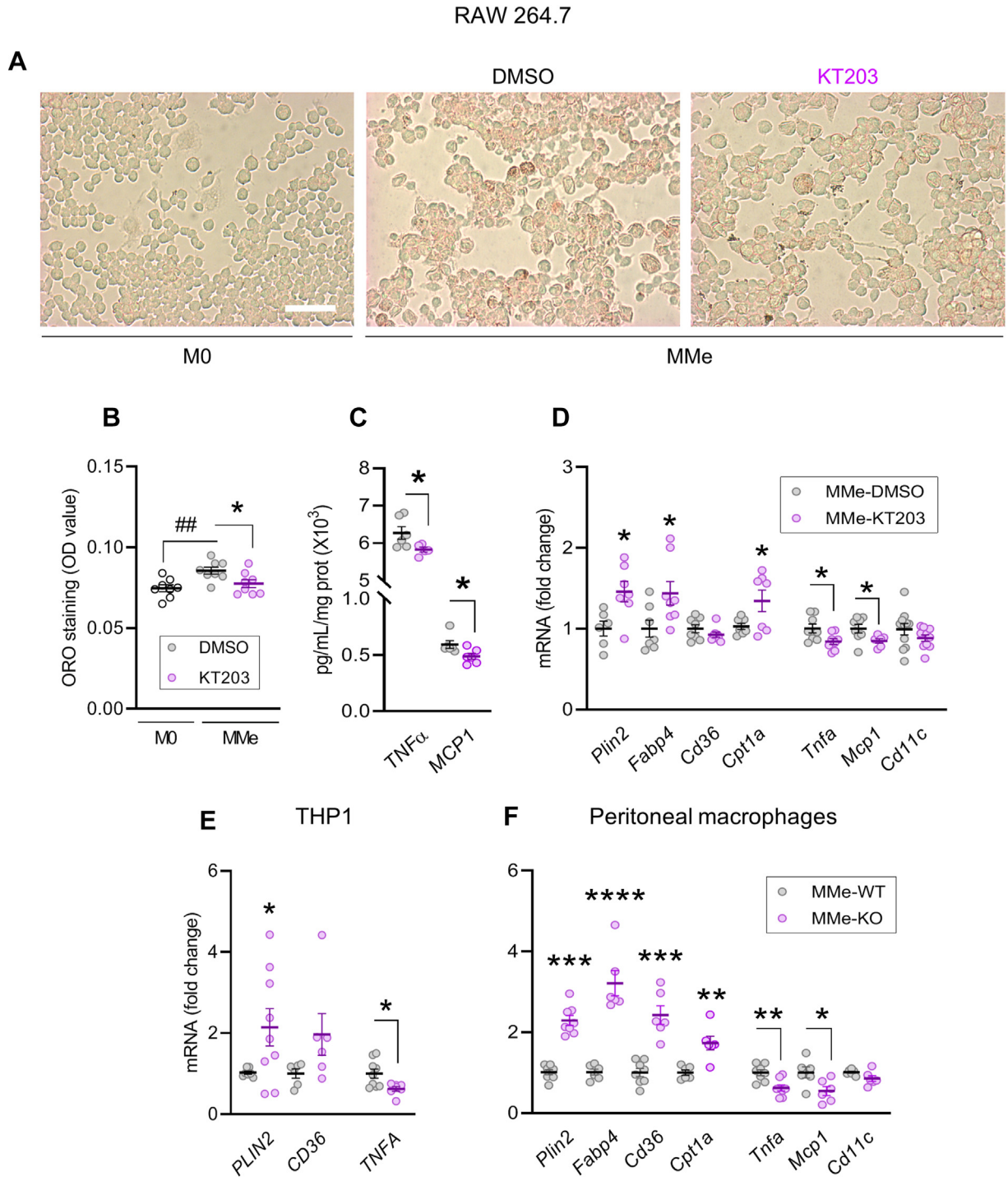

Figure 4: ABHD6 suppression or inhibition in MMe macrophages upregulates lipid metabolism genes and reduces pro-inflammatory markers. The M0 macrophages were polarized into MMe phenotype by treatment with glucose (30 mM) and insulin (10 nM) and palmitate (0.4 mM) for 24 h. ABHD6 inhibitor KT203 (10 μM) was added 1 h before the polarization treatments. **(A** and **B)** Representative images and quantity of oil red O staining. Scale bar: 100 um. **(C)** Cytokine release. **(D**–**F)** The mRNA levels of lipid metabolism and inflammatory genes. Minimum 6 mice/group. **(B)** One-way ANOVA and Tukey's post hoc test; **(C)** Mann Whitney test; **(D**–**F)** Student's t test; $^{*}p < 0.05$, $^{**}p < 0.01$, $^{***}p < 0.001$, $^{****}p < 0.0001$; $^{\#\#}p < 0.01$.

and PPAR target genes were examined in these conditions. Treatment of cells with 2-OG significantly reduced *Tnfa* expression, yet elevated the expression of MMe marker *Plin2,* a PPARγ target gene [13] and *Cpt1a,* a PPARα target gene [51], comparable with the effects of WY and Pio (Figure 5A).

Further, there was no significant changes in *Trem2* expression when MMe macrophages were stimulated with MAGs or PPAR agonists (Figure S5a). We next analyzed the different MAG species in the MMe macrophages with or without treatment with the ABHD6 inhibitor, KT203. As shown in Figure 5B, levels of different 1-MAG species were

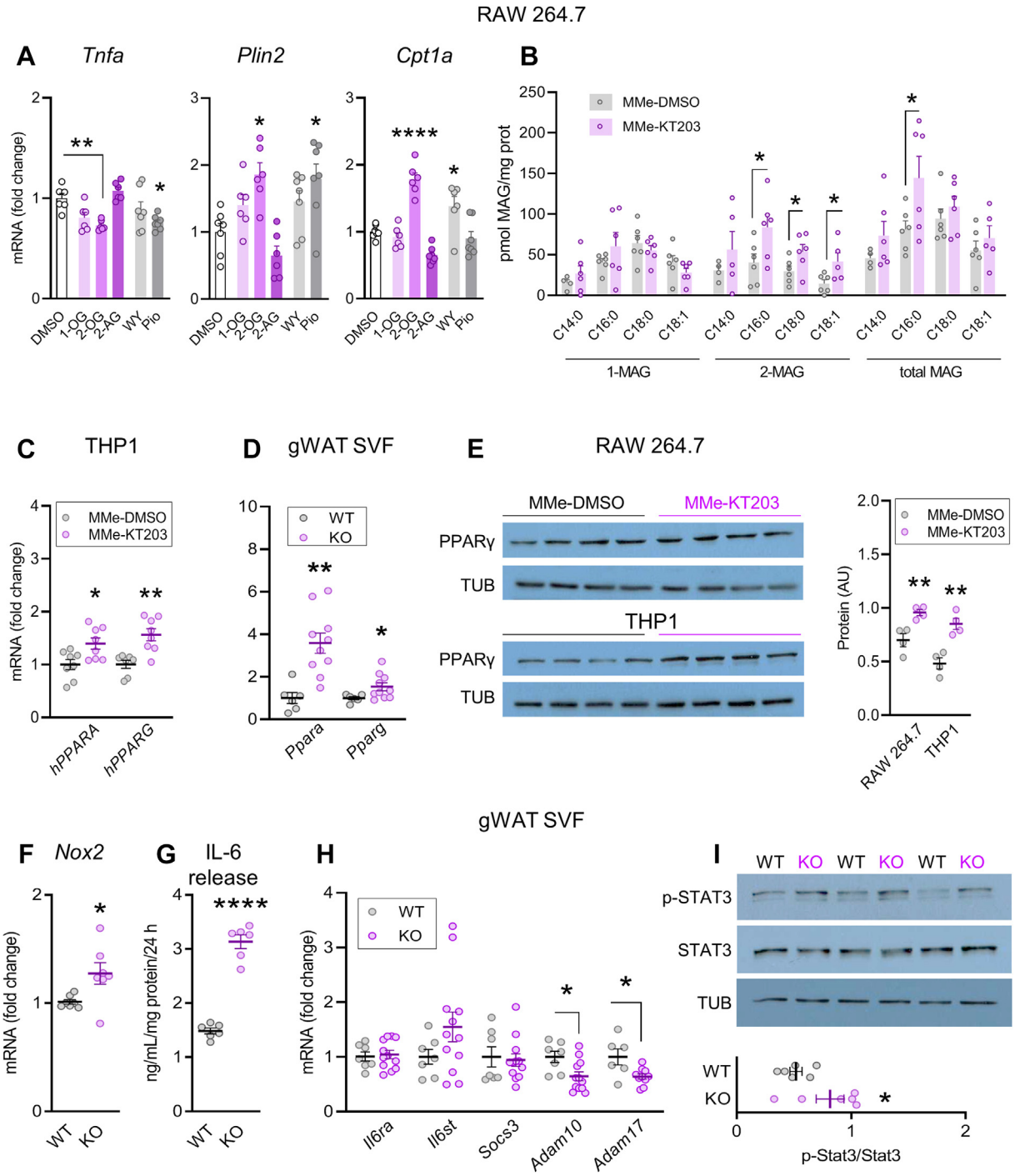

Figure 5: ABHD6 inhibition promotes 2MAG/PPARγ and α signaling in macrophages. The RAW264.7 macrophages (M0) were polarized into MMe phenotype by treatment with glucose (30 mM) and insulin (10 nM) and palmitate (0.4 mM) for 24 h. Exogenous MAGs or ABHD6 inhibitor KT203 (10 μM) were added 1 h before the polarization treatments. **(A)** Macrophages were treated with 10 μM MAG species (1-oleoylglycerol (1-OG), 2-OG and 2-Arachidonoylglycerol (2-AG)), as well as 50 μM PPARα (WY-14643 (WY)) or PPARγ (pioglitazone (Pio)) agonists for 24 h. The mRNA expressions of pro-inflammatory marker *Tnfa,* MMe marker *Plin2* (PPARγ target gene), and *Cpt1a* (PPARα target gene) were measured. **(B)** Analysis of 1-MAG, 2-MAG and total MAG species. **(C–E)** The mRNA and protein levels of PPARs. **(F)** *Nox2* mRNA level. **(G)** IL-6 release. **(H)** The mRNA levels of IL-6 signaling pathway components. **(I)** Western blot analysis of p-STAT3. **(A)** One-way ANOVA and Tukey's post hoc test; **(B–I)** Student's t test; $*p < 0.05$, $**p < 0.01$, $****p < 0.0001$.

unchanged by ABHD6 inhibition, but a significant augmentation in 2-MAG species (C16:0, C18:0, and C18:1) was observed in the KT203-treated versus control cells (Figure 5B). We have previously shown that 2-MAG [27], as well as 1-MAG [26], can activate PPARs. Accordingly, we found elevated mRNA expression of *Ppara* and *Pparg* in ABHD6-inhibited MMe human macrophage (THP1) cell-line (Figure 5C), gWAT-derived SVF from HFD-fed ABHD6-KO mice (Figure 5D). Enhanced protein expression of PPARγ was also observed

in KT203-treated murine and human macrophage cell-lines (Figure 5E), as compared to the corresponding controls.

Next, we aimed to evaluate the mechanistic link between 2-MAG/PPARs and enhanced anti-inflammatory M2 marker *Arg1* expression in the gonadal SVF of HFD-fed ABHD6-KO mice (Figure 2C). PPARα has been reported to be essential for NOX-induced oxidative stress in human and mouse macrophages [52]. Accordingly, as shown in Figure 5F, mRNA expression of *Nox2* was marginally, but significantly, enhanced in the gWAT SVF cells of HFD-fed ABHD6-KO mice, compared to the WT. Additionally, it was reported that MMe polarized ATMs from obese mice generate IL-6 in a NOX2-dependent manner [15]. Interestingly, we noticed that ABHD6-KO gWAT SVF cells exhibited a striking increase in IL-6 release *ex vivo,* compared to WT (Figure 5G; $p < 0.0001$). It is noteworthy that IL-6 is a pleiotropic cytokine that displays pro-inflammatory properties when mediating its effects through the trans-signaling pathway via the proteolytic cleavage of IL-6Rα by ADAM10 and ADAM17, and exerts anti-inflammatory effects through a classic signaling pathway [53]. Based on our results, the increased secretion of IL-6 from ABHD6-KO gWAT SVF appeared to elicit anti-inflammatory properties through the classic signaling pathway, as it was associated with decreased levels of *Adam10* and *Adam17* (Figure 5H). Because STAT3 activity was previously linked to IL-6 signaling and Arg1 expression in LPS-induced macrophages [54], we tested whether similar pathway is activated in ABHD6-deleted ATMs during obesity. In fact, we found increased STAT3 phosphorylation in gWAT SVF cells from ABHD6- KO mice versus WT (Figure 5I), highlighting a possible role of autocrine IL-6/STAT3 signaling in the anti-inflammatory effects of ABHD6 suppression.

Furthermore, iBAT-SVF from KO *vs.* WT also demonstrated enhanced expression of PPARs (Figure S5b), marginally increased IL-6 secretion (Figure S5d), and decreased *Adam10* and *Adam17* levels (Figure S5e), but without changes in *Nox2* (Figure S5c), and as shown earlier, no difference in *Arg1* mRNA expression (Figure 2D). Finally, the negligible phenotype observed in the KO inguinal depot was consistent with lack of alterations in PPARs levels and IL-6 release from iWAT-SVF (Figure 5f and g). Overall, our data support the involvement of a novel immunometabolic pathway 2-MAG/PPARs-NOX2/IL-6/STAT3/Arg1, which favors the anti-inflammatory state of gWAT-SVF in obesity.

4. DISCUSSION

The current *in vitro* and *in vivo* studies demonstrate that ABHD6 plays a pro-inflammatory role under metabolic nutri-stress conditions. Besides, our data show that global deletion of ABHD6 curtails the adipose and systemic pro-inflammatory responses to high-fat feeding. This led us to uncover an endogenous macrophage lipolysis/ABHD6/2-MAG/PPAR axis that acts as an immunometabolic network and favors anti-inflammatory polarization of gWAT ATMs in obesity.

Here we have studied the link between ABHD6 and chronic inflammation in the context of obesity. To our knowledge, this is the first report showing the favorable effect of lipolytic-derived 2-MAG species in ATM reprogramming to harbor enhanced lipid metabolism and decreased pro-inflammatory features in obesity. In contrast to the pro-inflammatory roles of fat resident macrophages, it is now accepted that during obesity certain subsets of ATMs maintain AT health and promote adipocyte turnover by taking-up excess FFAs and clearing the dead fat cells [14,55,56]. Thus, the lipid metabolism components, which were highly increased in ABHD6-inhibited/deleted MMe macrophages/gWAT SVF, may enable these cells to appropriately buffer their environment from excessive lipids while maintaining cell health. In fact, the observed reduced lipid (TG) content of ABHD6-suppressed MMe and ABHD6-KO iBAT-SVF, in parallel with enhanced lipolytic activity of the KO mature adipocytes, suggests a high rate of lipid metabolism in ABHD6-suppressed ATM/MMe. Noteworthy, enhanced ATM lipophagy, independent of their inflammatory phenotype, has been associated with lower ATM lipid content and increased AT lipolysis [57,58]. The possible involvement and impact of autophagy/lipophagy processes in ABHD6-deleted ATM requires further studies.

What is the evidence for the role of a macrophage lipolysis/2-MAG/PPARγ and α axis in modulating the phenotype of ATMs upon ABHD6 inhibition or suppression? We previously reported that ABHD6 suppression in pancreatic islets or adipose tissues results in the accumulation of intracellular MAG species [24,26,27]. In the current study, ABHD6 suppression reduced SVF lipolysis, as evidenced by reduced glycerol and FFA release, consistent with the fact that this enzyme contributes to the last step of lipolysis. MAG analysis of MMe macrophages showed elevated 2-MAG species in KT203-treated versus untreated cells. Further, we have recently shown that 2-MAG (in particular 2-OG) strongly enhances PPARα transactivation [27]. Here, *in vitro* treatment of MMe macrophages with exogenous 2-OG resulted in the downregulation of M1 markers and upregulation of PPARγ/α target genes. Accordingly, the results showed increased mRNA and protein expression of PPARγ and PPARα and their target genes in ABHD6 inhibited MMe macrophages, as well as in SVF cells of gWAT and iBAT from HFD-fed ABHD6-KO mice. Thus, these data provide strong evidence that suppression of ABHD6 in MMe macrophages leads to the accumulation of 2-MAG species, but not 1-MAG, which likely results in PPARs activation, as evidenced by enhanced levels of PPAR target genes and decreased inflammation. This view is consistent with the known anti-inflammatory effects of PPARs activators on macrophage phenotype under different pathological and inflammatory conditions [59,60].

With respect to the involvement of a NOX2/IL-6/STAT3/Arg1 signaling cascade in the anti-inflammatory effects of ABHD6 suppression, PPARα agonists were shown to increase macrophage ROS production through elevated expression of NADPH oxidases (NOX), which leads to the formation of lipid metabolites that exert anti-inflammatory PPARα—dependent responses in rodents and human macrophages [52]. Consistently, our data reveal parallel increase of *Ppara* and *Nox2* expression in gWAT SVF cells of HFD-fed KO vs WT mice. Further, it was recently reported that obesity-associated MMe macrophages release IL-6 in a NOX2-dependent manner [15]. Accordingly, we found enhanced secretion of IL-6 from KO gWAT SVF versus WT in an anti-inflammatory manner. Thus, the current data support the recent report [15] regarding the possible association of NOX2 with the IL-6 release from MMe macrophages. However, as the increase in *Nox2* expression in the KO gWAT-SVF was only $\sim$1.25-fold ($p = 0.02$) and the corresponding increase in IL-6 release was more than 2-fold ($p < 0.0001$) versus WT, we cannot rule out the possible contribution of other pathways that may induce IL6 release in absence of ABHD6. Further, the increased autocrine IL-6 production may have resulted in induction of *Arg1* expression and STAT3 phosphorylation known to modulate the *Arg1* gene [54]. Indeed, several recent studies have provided evidence for the beneficial metabolic and anti-inflammatory actions of IL-6 in white fat depots [61—63]. Overall, we propose that the beneficial effects of ABHD6 deletion in nutri-stress macrophages relies on 2-MAG/PPARs signaling, which limits pro-inflammatory responses (pro-inflammatory markers/cytokine release), enhances lipid metabolism (PPARγ target genes: *Fabp4*, *Plin2*, and *Cd36*) and basal respiratory capacity, and possibly activates the downstream anti-inflammatory NOX2/IL-6/STAT3/Arg1 cascade (Figure 6). Therefore, our findings identify ABHD6 as a key component of pro-inflammatory pathways in

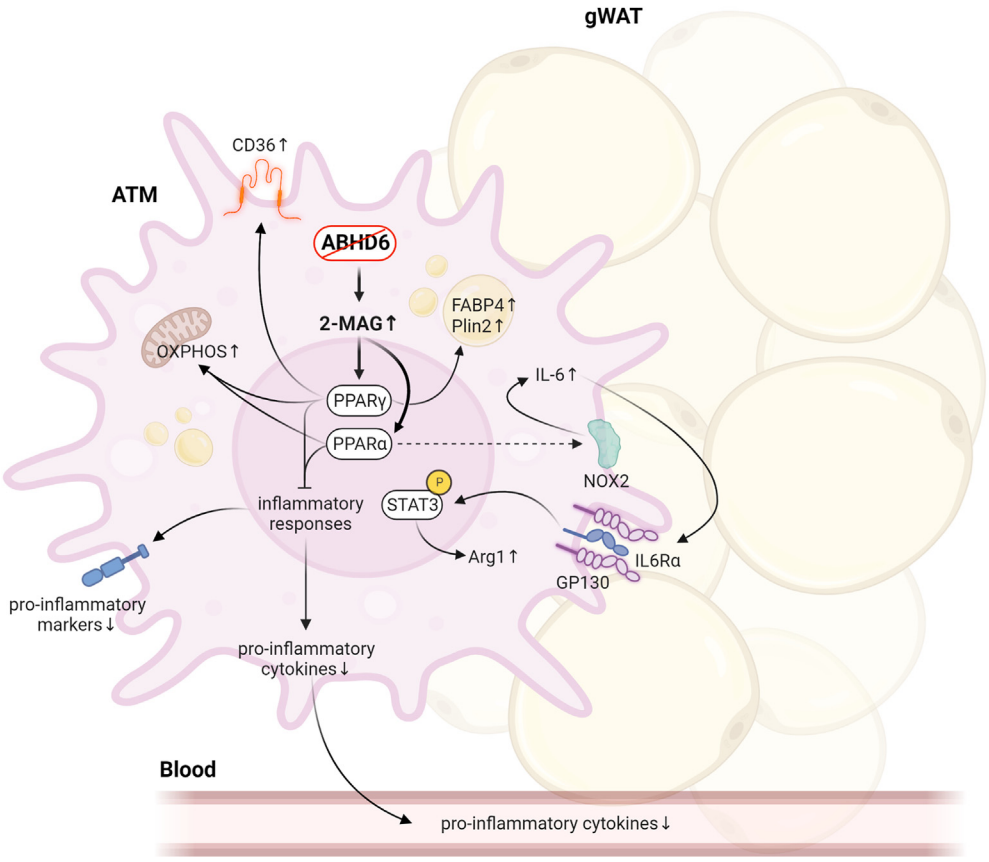

Figure 6: ABHD6 deletion attenuates obesity-related inflammation of gWAT ATMs by promoting anti-inflammatory pathways. Suppression of ABHD6 leads to the accumulation of 2-monoacylglycerol (2-MAG) species in nutri-stress macrophages, which results in peroxisome proliferator-activated receptors (PPARs) activation, and thus enhanced levels of PPAR target genes (*Fabp4*, *Plin2*, and *Cd36*) and basal respiratory capacity, and decreased inflammation. Also, PPARα activation possibly activates the downstream anti-inflammatory NADPH-oxidase-2 (NOX2)/interleukin-6 (IL-6)/signal transducer and activator of transcription 3 (STAT3)/arginase 1 (Arg1) cascade.

ATMs of obese mice, and that its suppression activates anti-inflammatory/lipid metabolism pathways to counterbalance the obesity-induced pro-inflammatory programs.

A limitation of the current study is the use of whole-body ABHD6-KO mouse model only, which does not allow us to definitively rule out, *in vivo*, the possible involvement of other tissues or other cells within the SVF fraction, other than macrophages, in the beneficial action of ABHD6 suppression. Even though an additional macrophage-specific ABHD6-KO mouse model can be useful in delineating the role of macrophage ABHD6, *in vivo*, the exhaustive *in vitro* work in both mouse and human macrophages using pharmacological and genetic approaches entirely support our conclusions. With regard to the clinical implication of these findings, further studies are required to assess if ABHD6 can serve as a diagnostic biomarker in inflammatory diseases. Indeed, the expression of ABHD6 is known to be elevated in the lymphoblastoid cells of European donors with systemic lupus erythematosus [64,65]. In addition, our findings support a model wherein ABHD6-deleted gWAT-SVF cells exhibit an activation of anti-inflammatory NOX2/IL-6/STAT3/Arg1 pathway. However, additional work, employing tissue-specific knockout models, may be required to fully demonstrate the direct link between 2-MAG/PPARs and the NOX2/IL-6/STAT3/Arg1 pathway.

In summary, the current study demonstrates that ABHD6 is a novel determinant of macrophage polarization and systemic inflammation during nutritional stress with high-fat feeding. We propose that during obesity-induced chronic low grade inflammatory condition, i.e. in the presence of elevated circulating lipids, ABHD6 suppression limits pro-inflammatory and activates anti-inflammatory pathways in macrophages. Finally, we report a novel endogenous ATM lipolysis/ABHD6/2-MAG/PPARs-associated lipid signaling and immunometabolic pathway in gWAT that plays a protective role in response to obesity-induced inflammation.

AUTHOR CONTRIBUTIONS

PP, SRMM, and MP designed research; PP, CS, IC, YHL, AKO, YB, LLK, AA, and RL performed research; PP, CS, MAF, JA, FAM, MLP, SRMM, and MP analyzed data; and PP, SRMM, and MP wrote the paper.

DATA AVAILABILITY

Data will be made available on request.

ACKNOWLEDGMENTS

This study was supported by funds from the Canadian Institutes of Health Research (#143308 to M.*P. and* S.R.M.M.) and Dasman Diabetes Research Institute/Montreal Medical International (to M.P., S.R.M.M., M.A-F., J.A., F.A-M.). M.P. was recipient up to

2019 of a Canada Research Chair in Diabetes and Metabolism. P.P. was recipient of postdoctoral fellowships from the Fondation Valifonds, the Montreal Diabetes Research Center, the CRCHUM and Mitacs. We thank the animal facility and the core facilities infor Cellular Physiology, Metabolomics and Rodent Phenotyping of the CRCHUM/Montreal Diabetes Research Center. We thank Jennifer Estall (University of Montreal) for the p-STAT3/STAT3 antibodies. We also gratefully acknowledge Marc Donath (University of Basel) for helpful discussion. Figure 6 was created with BioRender.com.

DECLARATION OF COMPETING INTEREST

The authors declare that they have no known competing financial interests or personal relationships that could have appeared to influence the work reported in this paper.

APPENDIX A. SUPPLEMENTARY DATA

Supplementary data to this article can be found online at https://doi.org/10.1016/j.molmet.2023.101822.

REFERENCES

[1] Murray PJ, Wynn TA. Protective and pathogenic functions of macrophage subsets. Nat Rev Immunol 2011;11(11):723–37.
[2] Wynn TA, Chawla A, Pollard JW. Macrophage biology in development, homeostasis and disease. Nature 2013;496(7446):445–55.
[3] Murray PJ, Allen JE, Biswas SK, Fisher EA, Gilroy DW, Goerdt S, et al. Macrophage activation and polarization: nomenclature and experimental guidelines. Immunity 2014;41(1):14–20.
[4] Odegaard JI, Ricardo-Gonzalez RR, Goforth MH, Morel CR, Subramanian V, Mukundan L, et al. Macrophage-specific PPARgamma controls alternative activation and improves insulin resistance. Nature 2007;447(7148):1116–20.
[5] Hotamisligil GS. Inflammation, metaflammation and immunometabolic disorders. Nature 2017;542(7640):177–85.
[6] Wellen KE, Hotamisligil GS. Inflammation, stress, and diabetes. J Clin Invest 2005;115(5):1111–9.
[7] Olefsky JM, Glass CK. Macrophages, inflammation, and insulin resistance. Annu Rev Physiol 2010;72:219–46.
[8] Lumeng CN, Saltiel AR. Inflammatory links between obesity and metabolic disease. J Clin Invest 2011;121(6):2111–7.
[9] Lumeng CN, Bodzin JL, Saltiel AR. Obesity induces a phenotypic switch in adipose tissue macrophage polarization. J Clin Invest 2007;117(1):175–84.
[10] Wculek SK, Dunphy G, Heras-Murillo I, Mastrangelo A, Sancho D. Metabolism of tissue macrophages in homeostasis and pathology. Cell Mol Immunol 2022;19(3):384–408.
[11] Yang S, Bossche JVd, Ramalho T. Macrophage Metabolism at the Crossroad of Metabolic Diseases and Cancer. Immunometabolism 2020;2(3):e200022.
[12] Nance SA, Muir L, Lumeng C. Adipose tissue macrophages: Regulators of adipose tissue immunometabolism during obesity. Mol Metab 2022;66:101642.
[13] Kratz M, Coats BR, Hisert KB, Hagman D, Mutskov V, Peris E, et al. Metabolic dysfunction drives a mechanistically distinct proinflammatory phenotype in adipose tissue macrophages. Cell Metab 2014;20(4):614–25.
[14] Coats BR, Schoenfelt KQ, Barbosa-Lorenzi VC, Peris E, Cui C, Hoffman A, et al. Metabolically Activated Adipose Tissue Macrophages Perform Detrimental and Beneficial Functions during Diet-Induced Obesity. Cell Rep 2017;20(13):3149–61.
[15] Tiwari P, Blank A, Cui C, Schoenfelt KQ, Zhou G, Xu Y, et al. Metabolically activated adipose tissue macrophages link obesity to triple-negative breast cancer. J Exp Med 2019;216(6):1345–58.
[16] Vogel A, Brunner JS, Hajto A, Sharif O, Schabbauer G. Lipid scavenging macrophages and inflammation. Biochim Biophys Acta Mol Cell Biol Lipids 2022;1867(1):159066.
[17] Batista-Gonzalez A, Vidal R, Criollo A, Carreno LJ. New Insights on the Role of Lipid Metabolism in the Metabolic Reprogramming of Macrophages. Front Immunol 2019;10:2993.
[18] Serbulea V, Upchurch CM, Schappe MS, Voigt P, DeWeese DE, Desai BN, et al. Macrophage phenotype and bioenergetics are controlled by oxidized phospholipids identified in lean and obese adipose tissue. Proc Natl Acad Sci USA 2018;115(27):E6254–63.
[19] Boutens L, Stienstra R. Adipose tissue macrophages: going off track during obesity. Diabetologia 2016;59(5):879–94.
[20] Im SS, Yousef L, Blaschitz C, Liu JZ, Edwards RA, Young SG, et al. Linking lipid metabolism to the innate immune response in macrophages through sterol regulatory element binding protein-1a. Cell Metab 2011;13(5):540–9.
[21] Dennis EA, Deems RA, Harkewicz R, Quehenberger O, Brown HA, Milne SB, et al. A mouse macrophage lipidome. J Biol Chem 2010;285(51):39976–85.
[22] Poursharifi P, Madiraju SRM, Prentki M. Monoacylglycerol signalling and ABHD6 in health and disease. Diabetes Obes Metab 2017;19(Suppl 1):76–89.
[23] Blankman JL, Simon GM, Cravatt BF. A comprehensive profile of brain enzymes that hydrolyze the endocannabinoid 2-arachidonoylglycerol. Chem Biol 2007;14(12):1347–56.
[24] Zhao S, Mugabo Y, Iglesias J, Xie L, Delghingaro-Augusto V, Lussier R, et al. α/β-Hydrolase domain-6-accessible monoacylglycerol controls glucose-stimulated insulin secretion. Cell Metab 2014;19(6):993–1007.
[25] Zhao S, Poursharifi P, Mugabo Y, Levens EJ, Vivot K, Attane C, et al. alpha/beta-Hydrolase domain-6 and saturated long chain monoacylglycerol regulate insulin secretion promoted by both fuel and non-fuel stimuli. Mol Metab 2015;4(12):940–50.
[26] Zhao S, Mugabo Y, Ballentine G, Attane C, Iglesias J, Poursharifi P, et al. alpha/beta-Hydrolase Domain 6 Deletion Induces Adipose Browning and Prevents Obesity and Type 2 Diabetes. Cell Rep 2016;14(12):2872–88.
[27] Poursharifi P, Attané C, Mugabo Y, Al-Mass A, Ghosh A, Schmitt C, et al. Adipose ABHD6 regulates tolerance to cold and thermogenic programs. JCI Insight 2020;5(24):e140294.
[28] Alhouayek M, Masquelier J, Cani PD, Lambert DM, Muccioli GG. Implication of the anti-inflammatory bioactive lipid prostaglandin D2-glycerol ester in the control of macrophage activation and inflammation by ABHD6. Proc Natl Acad Sci USA 2013;110(43):17558–63.
[29] Naydenov AV, Horne EA, Cheah CS, Swinney K, Hsu KL, Cao JK, et al. ABHD6 blockade exerts antiepileptic activity in PTZ-induced seizures and in spontaneous seizures in R6/2 mice. Neuron 2014;83(2):361–71.
[30] Masquelier J, Alhouayek M, Terrasi R, Bottemanne P, Paquot A, Muccioli GG. Lysophosphatidylinositols in inflammation and macrophage activation: Altered levels and anti-inflammatory effects. Biochim Biophys Acta Mol Cell Biol Lipids 2018;1863(12):1458–68.
[31] Wen J, Ribeiro R, Tanaka M, Zhang Y. Activation of CB2 receptor is required for the therapeutic effect of ABHD6 inhibition in experimental autoimmune encephalomyelitis. Neuropharmacology 2015;99:196–209.
[32] Iglesias J, Lamontagne J, Erb H, Gezzar S, Zhao S, Joly E, et al. Simplified assays of lipolysis enzymes for drug discovery and specificity assessment of known inhibitors. J Lipid Res 2016;57(1):131–41.
[33] Tanaka M, Moran S, Wen J, Affram K, Chen T, Symes AJ, et al. WWL70 attenuates PGE(2) production derived from 2-arachidonoylglycerol in microglia by ABHD6-independent mechanism. J Neuroinflammation 2017;14(1):7.
[34] Prentki M, Peyot ML, Masiello P, Madiraju SRM. Nutrient-Induced Metabolic Stress, Adaptation, Detoxification, and Toxicity in the Pancreatic β-Cell. Diabetes 2020;69(3):279–90.
[35] Ter Horst R, van den Munckhof ICL, Schraa K, Aguirre-Gamboa R, Jaeger M, Smeekens SP, et al. Sex-Specific Regulation of Inflammation and Metabolic Syndrome in Obesity. Arterioscler Thromb Vasc Biol 2020;40(7):1787–800.
[36] Pettersson US, Waldén TB, Carlsson PO, Jansson L, Phillipson M. Female mice are protected against high-fat diet induced metabolic syndrome and increase the regulatory T cell population in adipose tissue. PLoS One 2012;7(9):e46057.

[37] Singer K, Maley N, Mergian T, DelProposto J, Cho KW, Zamarron BF, et al. Differences in Hematopoietic Stem Cells Contribute to Sexually Dimorphic Inflammatory Responses to High Fat Diet-induced Obesity. J Biol Chem 2015;290(21):13250–62.
[38] Estrany ME, Proenza AM, Gianotti M, Lladó I. High-fat diet feeding induces sex-dependent changes in inflammatory and insulin sensitivity profiles of rat adipose tissue. Cell Biochem Funct 2013;31(6):504–10.
[39] Li J, Ruggiero-Ruff RE, He Y, Qiu X, Lainez N, Villa P, et al. Sexual dimorphism in obesity is governed by RELMα regulation of adipose macrophages and eosinophils. eLife 2023;12:e86001.
[40] Zhang X, Goncalves R, Mosser DM. The isolation and characterization of murine macrophages. Curr Protoc Immunol Chapter 2008;14(14 11 11). 14:14 11 11-14 11 14.
[41] Cho KW, Morris DL, Lumeng CN. Flow cytometry analyses of adipose tissue macrophages. Methods Enzymol 2014;537:297–314.
[42] Stenkula KG, Erlanson-Albertsson C. Adipose cell size: importance in health and disease. Am J Physiol Regul Integr Comp Physiol 2018;315(2):R284–95.
[43] Ertunc ME, Hotamisligil GS. Lipid signaling and lipotoxicity in metaflammation: indications for metabolic disease pathogenesis and treatment. J Lipid Res 2016;57(12):2099–114.
[44] Gaidhu MP, Anthony NM, Patel P, Hawke TJ, Ceddia RB. Dysregulation of lipolysis and lipid metabolism in visceral and subcutaneous adipocytes by high-fat diet: role of ATGL, HSL, and AMPK. Am J Physiol Cell Physiol 2010;298(4):C961–71.
[45] de Luca C, Olefsky JM. Inflammation and insulin resistance. FEBS Lett 2008;582(1):97–105.
[46] Weisberg SP, McCann D, Desai M, Rosenbaum M, Leibel RL, Ferrante Jr AW. Obesity is associated with macrophage accumulation in adipose tissue. J Clin Invest 2003;112(12):1796–808.
[47] Jaitin DA, Adlung L, Thaiss CA, Weiner A, Li B, Descamps H, et al. Lipid-Associated Macrophages Control Metabolic Homeostasis in a Trem2-Dependent Manner. Cell 2019;178(3):686–698 e614.
[48] Prunet-Marcassus B, Cousin B, Caton D, André M, Pénicaud L, Casteilla L. From heterogeneity to plasticity in adipose tissues: site-specific differences. Exp Cell Res 2006;312(6):727–36.
[49] Huang SC, Everts B, Ivanova Y, O'Sullivan D, Nascimento M, Smith AM, et al. Cell-intrinsic lysosomal lipolysis is essential for alternative activation of macrophages. Nat Immunol 2014;15(9):846–55.
[50] Hsu KL, Tsuboi K, Chang JW, Whitby LR, Speers AE, Pugh H, et al. Discovery and optimization of piperidyl-1,2,3-triazole ureas as potent, selective, and in vivo-active inhibitors of α/β-hydrolase domain containing 6 (ABHD6). J Med Chem 2013;56(21):8270–9.
[51] Bougarne N, Weyers B, Desmet SJ, Deckers J, Ray DW, Staels B, et al. Molecular Actions of PPARα in Lipid Metabolism and Inflammation. Endocrine Reviews 2018;39(5):760–802.
[52] Teissier E, Nohara A, Chinetti G, Paumelle R, Cariou B, Fruchart JC, et al. Peroxisome proliferator-activated receptor alpha induces NADPH oxidase activity in macrophages, leading to the generation of LDL with PPAR-alpha activation properties. Circ Res 2004;95(12):1174–82.
[53] Scheller J, Chalaris A, Schmidt-Arras D, Rose-John S. The pro- and anti-inflammatory properties of the cytokine interleukin-6. Biochim Biophys Acta 2011;1813(5):878–88.
[54] Dichtl S, Lindenthal L, Zeitler L, Behnke K, Schlosser D, Strobl B, et al. Lactate and IL6 define separable paths of inflammatory metabolic adaptation. Sci Adv 2021;7(26):eabg3505.
[55] Fitzgibbons TP, Czech MP. Emerging evidence for beneficial macrophage functions in atherosclerosis and obesity-induced insulin resistance. J Mol Med (Berl) 2016;94(3):267–75.
[56] Sun K, Kusminski CM, Scherer PE. Adipose tissue remodeling and obesity. J Clin Invest 2011;121(6):2094–101.
[57] Xu X, Grijalva A, Skowronski A, van Eijk M, Serlie MJ, Ferrante Jr AW. Obesity activates a program of lysosomal-dependent lipid metabolism in adipose tissue macrophages independently of classic activation. Cell Metab 2013;18(6):816–30.
[58] Caslin HL, Bhanot M, Bolus WR, Hasty AH. Adipose tissue macrophages: Unique polarization and bioenergetics in obesity. Immunol Rev 2020;295(1):101–13.
[59] Straus DS, Glass CK. Anti-inflammatory actions of PPAR ligands: new insights on cellular and molecular mechanisms. Trends Immunol 2007;28(12):551–8.
[60] Gallardo-Soler A, Gómez-Nieto C, Campo ML, Marathe C, Tontonoz P, Castrillo A, et al. Arginase I induction by modified lipoproteins in macrophages: a peroxisome proliferator-activated receptor-gamma/delta-mediated effect that links lipid metabolism and immunity. Mol Endocrinol 2008;22(6):1394–402.
[61] Han MS, White A, Perry RJ, Camporez J-P, Hidalgo J, Shulman GI, et al. Regulation of adipose tissue inflammation by interleukin 6. Proc Natl Acad Sci USA 2020;117(6):2751–60.
[62] Li H, Dong M, Liu W, Gao C, Jia Y, Zhang X, et al. Peripheral IL-6/STAT3 signaling promotes beiging of white fat. Biochim Biophys Acta Mol Cell Res 2021;1868(10):119080.
[63] Yu H, Dilbaz S, Coßmann J, Hoang AC, Diedrich V, Herwig A, et al. Breast milk alkylglycerols sustain beige adipocytes through adipose tissue macrophages. J Clin Invest 2019;129(6):2485–99.
[64] Oparina NY, Delgado-Vega AM, Martinez-Bueno M, Magro-Checa C, Fernández C, Castro RO, et al. PXK locus in systemic lupus erythematosus: fine mapping and functional analysis reveals novel susceptibility gene ABHD6. Ann Rheum Dis 2015;74(3):e14.
[65] Rahaman O, Bhattacharya R, Liu CSC, Raychaudhuri D, Ghosh AR, Bandopadhyay P, et al. Cutting Edge: Dysregulated Endocannabinoid-Rheostat for Plasmacytoid Dendritic Cell Activation in a Systemic Lupus Endophenotype. J Immunol 2019;202(6):1674–9.

